THE JOURNAL OF COMPARATIVE NEUROLOGY 440:109–125 (2001)

Morphology and Physiology of the Polyaxonal Amacrine Cells in the Rabbit Retina

BÉLA VÖLGYI,[1] DAIYAN XIN,[1] YIMY AMARILLO,[2] AND STEWART A. BLOOMFIELD[1,2]*
[1]Department of Ophthalmology, New York University School of Medicine, New York, New York 10016
[2]Department of Physiology and Neuroscience, New York University School of Medicine, New York, New York 10016

ABSTRACT

We examined the morphology and physiological response properties of the axon-bearing, long-range amacrine cells in the rabbit retina. These so-called polyaxonal amacrine cells all displayed two distinct systems of processes: (1) a dendritic field composed of highly branched and relatively thick processes and (2) a more extended, often sparsely branched axonal arbor derived from multiple thin axons emitted from the soma or dendritic branches. However, we distinguished six morphological types of polyaxonal cells based on differences in the fine details of their soma/dendritic/axonal architecture, level of stratification within the inner plexiform layer (IPL), and tracer coupling patterns. These morphological types also showed clear differences in their light-evoked response activity. Three of the polyaxonal amacrine cell types showed on-off responses, whereas the remaining cells showed on-center responses; we did not encounter polyaxonal cells with off-center physiology. Polyaxonal cells respected the on/off sublamination scheme in that on-off cells maintained dendritic/axonal processes in both sublamina *a* and *b* of the IPL, whereas processes of on-center cells were restricted to sublamina *b*. All polyaxonal amacrine cell types displayed large somatic action potentials, but we found no evidence for low-amplitude dendritic spikes that have been reported for other classes of amacrine cell. The center-receptive fields of the polyaxonal cells were comparable to the diameter of their respective dendritic arbors and, thus, were significantly smaller than their extensive axonal fields. This correspondence between receptive and dendritic field size was seen even for cells showing extensive homotypic and/or heterotypic tracer coupling to neighboring neurons. These data suggest that all polyaxonal amacrine cells are polarized functionally into receptive dendritic and transmitting axonal zones. J. Comp. Neurol. 440: 109–125, 2001.

Indexing terms: retina; amacrine cells; morphology; axons; coupling

The amacrine cells are the major interneurons in the proximal retina of vertebrates. It has been suggested that between 20 and 30 morphological subpopulations of amacrine cell exist in the mammalian retina, based on differences in somatic and dendritic architecture (Wässle and Boycott, 1991; MacNeil et al., 1999). The dendritic branches of these subtypes stratify within restricted levels of the inner plexiform layer (IPL), indicating selectivity in the synaptic connections made with bipolar cell axon terminals as well as the dendritic processes of neighboring amacrine and ganglion cells. It is believed that the structural diversity within the amacrine cell population reflects an equally large range of physiological properties corresponding to the functional roles amacrine cells play in formulating the retinal output signals expressed by the postsynaptic ganglion cells.

Interestingly, the amacrine cells were named by Ramón y Cajal (1893) after a Greek derivation of "neurons lacking long fibers," based on the typically circumscribed space occupied by their dendritic arbors. Yet, he also observed

*Correspondence to: Dr. Stewart Bloomfield, Department of Ophthalmology, NYU Medical Center, 550 First Avenue/MSB181, New York, NY 10016. E-mail: blooms01@med.nyu.edu

Received 16 May 2001; Revised 6 August 2001; Accepted 14 August 2001

amacrine cells in the reptilian and avian retinas with long processes that extended beyond a classic dendritic arbor. More contemporary studies have detailed a number of long-range amacrine cells with broad dendritic arbors spanning hundreds of microns across the retina (Kolb et al., 1981; Vaney, 1990; MacNeil et al., 1999). Further, a number of neurons with somata lying within the proximal inner nuclear layer (INL), ganglion cell layer (GCL), or even within the IPL have been described in mammals with very long, narrow axon-like processes distinct from a conventional dendritic arbor (Rodieck, 1988; Dacey, 1989, 1990; Famiglietti, 1992a,b,c; Freed et al., 1996). In contrast to ganglion cells, these so-called polyaxonal amacrine cells bear multiple axon-like fibers that emerge from the soma or dendritic processes and course for several millimeters through the IPL, but do not exit the retina. Clear morphological distinctions have been made between polyaxonal cells, both within and across species, indicating that they form a unique, yet varied, amacrine cell type in mammalian retina.

The function of polyaxonal cells, as for most other amacrine cell types, remains elusive. The separate dendritic and axonal arbors suggest a division of labor whereby the cell may be made up of electrically isolated, independent zones, each maintaining input and output synapses (Miller and Bloomfield, 1983). It has been suggested that the dendrites form a synaptic recipient zone, whereas the axon propagates this signal centrifugally to distant cells. This idea is supported by the finding that the size of the center-receptive fields of certain polyaxonal cells corresponds to that of their dendritic arbors, suggesting that the axons serve to distribute signals peripherally (Taylor, 1996; Stafford and Dacey, 1997). In contrast, however, polyaxonal cells in the cat retina display receptive fields about four times larger than the corresponding dendritic fields, suggesting that axons can convey peripheral signals to the soma (Freed et al., 1996). Unfortunately, ultrastructural data from polyaxonal cells are limited. Whereas presynaptic and postsynaptic specializations have been localized to dendritic processes (Famiglietti, 1992c; Freed et al., 1996), the synaptic contacts of the axons have yet to be elucidated. Thus, the relationship between the dendritic and axonal structures of polyaxonal cells in terms of signal reception and transmission remains unclear.

In the rabbit retina, Famiglietti (1992a,b,c) described four distinct subpopulations of polyaxonal amacrine cells, based on an analysis of Golgi and Nissl-stained material. Besides clear differences in soma size and location, these types were also differentiated by the strata in which their dendritic and axonal processes lay in the IPL. The four subtypes showed largely different levels of stratification, again suggesting that they maintain connections with different cell types and thereby likely express different physiological response properties. In the sole physiological study of rabbit polyaxonal amacrine cells, Taylor (1996) reported spiking cells with circumscribed on-center receptive fields and antagonistic off-surrounds. Unfortunately, this study was limited in scope and cells were not identified according to Famiglietti's classification scheme.

In the present study, we combined intracellular recordings with Neurobiotin labeling to allow for direct correlations between the structure and physiological response properties of the polyaxonal amacrine cells in the rabbit retina. Our goals in undertaking this systematic study were (1) to differentiate subpopulations of polyaxonal cells based on differences in somatic, dendritic, and axonal architecture and tracer-coupling patterns and (2) to determine similarities and differences between the response properties of these subpopulations. Based on these morphological criteria, we classified polyaxonal cells in the rabbit retina into six distinct categories. Further, although we found some physiological parameters common to all polyaxonal cells, others, such as response waveform and on/off organization, were largely stereotypic for the individual cell groups within our classification scheme.

MATERIALS AND METHODS

Preparation

The general methods used in this study have been described previously (Bloomfield and Miller, 1982; Bloomfield, 1992). All procedures were approved by the Institutional Animal Care and Use Committee at NYU School of Medicine. Briefly, adult Dutch-belted rabbits (1.5–2.5 kg) were anesthetized with an intraperitoneal injection of ethyl carbamate (2 g/kg body weight) and a local injection of 2% lidocaine hydrochloride to the eyelids and surrounding tissue. The eye was removed under dim red illumination and hemisected. The vitreous humour was removed with an ophthalmic sponge and the resultant retina-eyecup was mounted in a superfusion chamber. The chamber was then placed in a light-tight Faraday cage and superfused at a flow rate of 30 ml/min with a mammalian Ringer's solution (Bloomfield and Miller, 1982) or Ames medium (Sigma, St. Louis, MO). The superfusate was kept at a constant temperature of 35°C with oxygenation and pH 7.4 was maintained by bubbling with a gaseous mixture of 95% O_2- 5% CO_2. Retinas were maintained in complete darkness for approximately 45 minutes prior to initiation of recordings. Following enucleations, animals were killed with an intracardial injection of ethyl carbamate (5 ml of a 15% solution).

Light stimulation

Two 100-W quartz-iodide lamps provided white light for a dual-beam optical bench. Light intensity could be reduced up to 7 log units with calibrated neutral density filters placed in the light path of both beams. The maximum irradiance of both beams was equalized at 2.37 mW/cm^2 as measured by a radiometer placed in the same position in the light pathway normally occupied by the retina-eyecup. The beams were combined with a collecting prism and focused onto the vitreal surface of the retina-eyecup by means of a final focusing lens. The bottom beam was used for receptive field measures and provided small concentric spot stimuli (75 μm to 6.0 mm in diameter) as well as a 50 μm-wide/6.0 mm-long rectangular slit of light that was moved along its minor axis (parallel to the visual streak) in steps as small as 3 μm. Alignment of the electrode tip with stimuli was accomplished visually with the aid of a dissection microscope mounted in the Faraday cage. However, after impaling a neuron, the spot stimulus that evoked the largest amplitude, center-mediated response was considered centered over the cell and adjustment of the stimulus position was made accordingly.

Electrical recordings

Intracellular recordings were obtained from neurons with standard glass microelectrodes (outer diameter [o.d.]

= 1.2 mm, inner diameter [i.d.] = 0.6 mm). Electrodes were filled at their tips with 4% N-(2-amino-ethyl)-biotinamide hydrochloride, Neurobiotin (Vector Labs, Burlingame, CA) in 0.1 M Tris buffer (pH 7.6), and then back filled with 4 M potassium chloride. The final d.c. resistances of the electrodes ranged from 250 to 500 MΩ. Following physiological characterization of a cell, Neurobiotin was iontophoresed into the neuron using a combination of sinusoidal (3 Hz, 0.8 nA peak to peak) and d.c. current (0.4 nA) applied simultaneously; this method allowed passage of tracer through the electrode without polarization. Standardized injection and incubation times for the cells were based on a detailed, previous study made in our lab of the tracer coupling between horizontal cells in the rabbit retina (Bloomfield et al., 1995). Recordings were displayed on an oscilloscope, recorded on magnetic tape, and digitized off-line for computer analyses.

Receptive field measurements

To measure the center-receptive field of a cell, the 50 μm-wide/6.0 mm-long rectangular slit of light was moved along its minor axis (parallel to the visual streak) in discrete steps in both directions from the central position (Bloomfield, 1992). The position of the slit at which it evoked the largest amplitude response was considered being centered over the cell. Peak response amplitudes of slow potentials were plotted against stimulus position and the extent of a neuron's center-receptive field was taken to be the diameter of the Gaussian function fit to the data (Origin, Microcal, Northampton, MA). The Gaussian diameter was defined as 0.849 times the width (w) of the Gaussian at half height ($w \approx 2\sigma$). Area summation measurements were made by comparing peak responses to concentric spots of light with increasing diameters (175–3,600 μm), but constant intensity.

Histology

Following electrophysiological experimentation, retinas were fixed in a cold (4°C) solution of 4% paraformaldehyde-0.1% glutaraldehyde in 0.1 M phosphate buffer (pH 7.3) for 12 minutes. The retinas were then detached, trimmed, and fixed overnight at 4°C in the same fixative. They were washed in phosphate buffer and then reacted with the Elite ABC kit (Vector Labs) and 1% Triton-X in 10 mM sodium phosphate-buffered saline (9% saline, pH 7.6). Retinas were then processed for peroxidase histochemistry using 3-3' diaminobenzidine (DAB), dehydrated, cleared, and flatmounted. Images of labeled neurons were captured by a cooled CCD camera (Spot 2, Diagnostic Instruments, Sterling Heights, MI) followed by software manipulation of brightness and contrast (Photoshop, Adobe Systems, San Jose, CA). Drawings of cells were made using a camera lucida microscope attachment and then digitized by scanner and entered into a computer for reconstruction.

To determine the level at which dendritic and axonal processes stratified in the IPL, we examined Neurobiotin-labeled cells in flatmount under a 100× oil-immersion lens. The borders of the IPL were determined by the location of amacrine and ganglion cell bodies using Nomarski interference contrast optics. The position of the outer margin of the IPL next to the amacrine cell bodies was defined as 0, whereas the vitreal border of the IPL was defined as 100. The position of cellular processes in the IPL was determined using a precision micrometer and given a value from 0 to 100. Mutliple measures were made for a single cell to elucidate any variations in stratification throughout its extent.

RESULTS

Identification of polyaxonal cells

The data in this study come from recordings from over 100 long-range amacrine cells that were subsequently labeled with Neurobiotin and found to maintain dendritic/axonal arbors extending over 1 mm. All cells classified here as polyaxonal amacrine cells showed distinct dendritic and axonal arborizations in the IPL. In addition, all cellular impalements were made within the visual streak region corresponding to eccentricities of 0.5–2.8 mm from the optic disk.

The polyaxonal amacrine cells in this study were differentiated into morphological classes based on established criteria including (1) dendritic/axonal architecture including the level of stratification in the IPL; (2) soma size, shape, and position; and (3) tracer coupling pattern. Using these criteria, we have differentiated six morphological types of polyaxonal cells in the rabbit retina. In the sections below, we have chosen to describe first the morphology of these polyaxonal cell classes and then their corresponding physiology to facilitate direct comparisons between the structure and the light-evoked responses of these neurons.

Morphology of polyaxonal cells

Type I cells. The most common type of polyaxonal cell we encountered showed relatively large somata with diameters of 12–15 μm (Fig. 1). These somata were basically spherical in shape although many were elongated, particularly those that emitted primary dendrites at opposite poles (Fig. 1B). In addition, type I cell somata were found within the IPL, GCL, or the proximal portion of the INL. The dendritic arbor of these cells derived from two to four stout, 1.8–2.4-μm diameter primary branches and was made up of relatively smooth, highly wavy segments that showed up to fourth-order branching (Figs. 1B, 2A). The dendritic fields of type I cells ranged from 300 to 600 μm in diameter dependent on retinal eccentricity (Fig. 2A). The dendritic arbors broadly stratified within strata 2–4, but with most processes straddling the sublamina *a*/*b* border within the middle of the IPL.

Type I cells also showed slender (0.5–0.8 μm diameter), beaded axon-like processes that were emitted directly from the soma (Fig. 3B), or, more often, emerged at dendritic branchpoints (Figs. 1B, 3C). The axonal arbors of type I cells showed only occasional branching, but could be followed for several millimeters until segments faded gradually from view (Fig. 2A). Thus, the axonal arbors of these cells typically dwarfed their dendritic fields. The axonal arbor stratified mainly within strata 2–3 of the IPL, with some segments running slightly distally within stratum 1.

Type 1 polyaxonal amacrine cells showed a stereotypic tracer coupling pattern following injection with Neurobiotin; this included cells lying within the IPL, INL, or GCL. Injection of a single type I cell resulted in extensive tracer coupling of greater than 50 neighboring amacrine cells. These included cells within and somewhat beyond the space occupied by the dendritic arbor of the injected cell

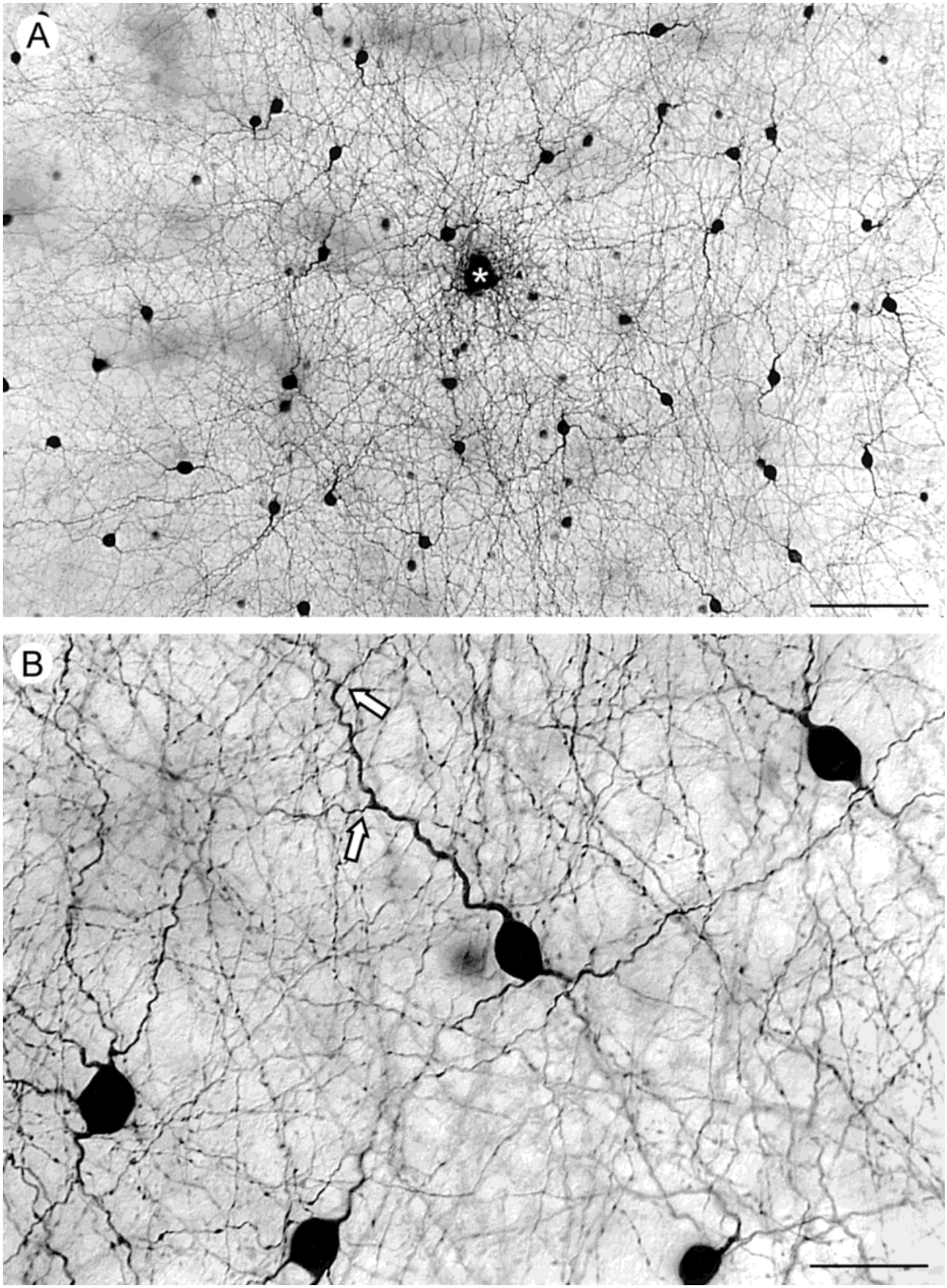

Fig. 1. **A:** Photomicrograph showing the extensive homologous and heterologous tracer-coupling pattern seen following injection of Neurobiotin into a single type I polyaxonal amacrine cell. Asterisk shows the injection site. **B:** Higher-power photomicrograph demonstrates the somata of tracer-coupled type I polyaxonal cells within the inner plexiform layer (IPL) and the overlapping dendritic and axonal arbors of neighboring cells. Arrows indicate axonal processes emerging from proximal dendrites. Scale bar = 100 μm in A, 25 μm in B.

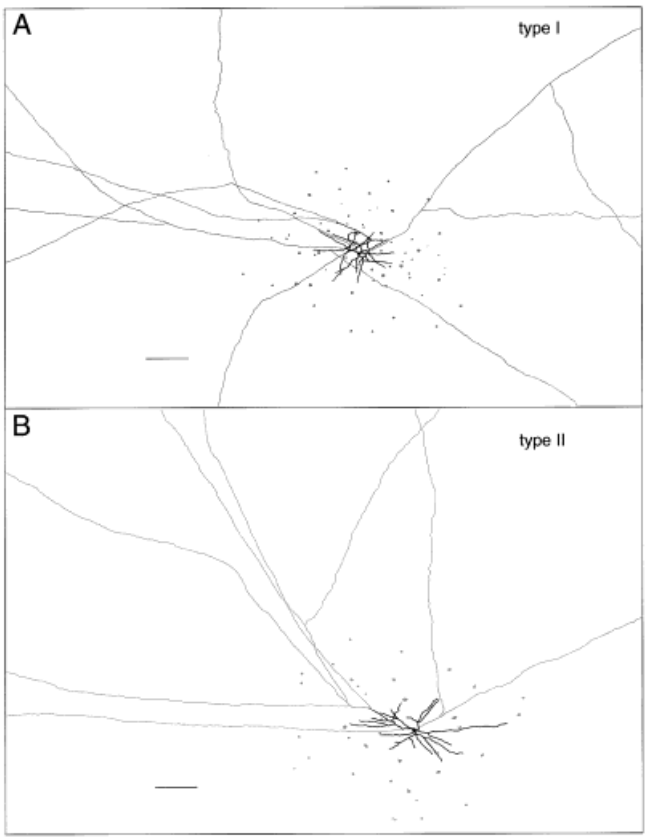

Fig. 2. **A:** Camera lucida drawing providing a flatmount view of a type I polyaxonal cell labeled with Neurobiotin. The dendritic arbor is presented in black, whereas the axonal arbor and the somata of tracer-coupled cells are presented in gray. **B:** Camera lucida drawing of a type II polyaxonal cell showing the dendritic and axonal systems as well as the somata of tracer-coupled cells. Conventions are the same as in A.

(Fig. 2A). However, all tracer-coupled cells were close enough so that coupling could be achieved by dendritic-dendritic interactions only. Most of the tracer-coupled cells were labeled darkly and shared the somatic and dendritic profile of the injected cell indicating homologous coupling (Fig. 1). These coupled type I cell somata were found within the IPL, GCL, or the proximal INL. However, other tracer-coupled amacrine cells (soma diameters of 6–8 μm) were labeled more lightly and, moreover, showed somatic and dendritic architecture distinct from that of type I cells (Figs. 3A,C). These data suggest that type 1 polyaxonal cells are heterologously coupled to at least three different types of amacrine cell. One of these heterologously coupled cells showed somatic/dendritic architecture resembling that of the type II polyaxonal cells described below (Fig. 3C). In addition, a few lightly labeled somata, 15–20 μm in diameter, were often seen in the GCL and are presumed to be coupled ganglion cells. However, these ganglion cell somata often formed a sparse, irregular array that was usually close to the injection site. Therefore, it is unclear whether they reflect true tracer coupling or artifactual staining from tracer leaked out of electrode as it was advanced through the proximal retina.

Type II cells. The second type of polyaxonal amacrine cell maintained oval somata, about 12 μm in diameter, which lay within the proximal portion of the INL (Fig. 4). A distinctive feature of type II cells was a single, primary dendritic stalk that plunged into the middle of the IPL and then divided into two main branches, each about 2 μm in diameter, that further divided to produce the dendritic arbor (Fig. 4B). The dendrites of type II cells were smooth and less wavy than those of type I polyaxonal cells. Their dendritic arbors were often elongated along the axis parallel to the visual streak, extending 300–600 μm along this axis (Fig. 2B). Similar to type I cells, the dendrites of type II amacrine cells stratified within strata 2–4 of the IPL. A separate axonal arbor was formed by thin, beaded segments that emerged as side branches from dendrites (Fig. 4A) or directly from the cell body (Fig. 4C). Again, the axonal arbor could be followed for several millimeters before processes faded from view. Interestingly, the axonal arbor of type II cells stratified distal to the dendritic arbor within strata 1–3 of the IPL, although there was considerable overlap between the two.

Type II cells showed only homologous tracer coupling (Fig. 4A). As mentioned above, injections of Neurobiotin into type I polyaxonal cells occasionally labeled neurons matching the description of type II cells. It is therefore curious that we did not see movement of tracer in the opposite direction. Although this difference in tracer coupling pattern may indicate rectifying gap junctions between type I and II cells, misidentification of heterologously coupled cells as type II neurons following type I cell injections cannot be ruled out.

Type III cells. All of the tracer injections we made of type III cells resulted in a large accumulation of extracellular label that obscured the somata of injected cells. Therefore, details about the cell bodies of these type neurons were inferred from the profiles of tracer-coupled cells. All injected type III cells lay in the GCL and were tracer coupled to three to five cells laying in both the GCL and proximal INL. The somata of the coupled cells in both layers were spherical and medium sized, 10–12 μm in diameter. It is therefore unclear whether the cells labeled in the INL reflect heterologous coupling or mirror-symmetric type III cells. Two or three main dendrites were emitted from the cell body to form a dendritic arbor running from 350 to 500 μm across (Fig. 5A). The dendrites of type III cells were highly irregular, showing numerous varicosities, spines, short side-appendages, and tortuously wavy segments (Figs. 6A,B). The spine profiles projected orthogonally from the dendritic branches and showed varied architecture: shorter spines ended in terminal boutons, whereas the longer spines were more slender and maintained a more uniform caliber along their lengths (Fig. 6B). The dendritic arbor of type III cells stratified within strata 2–4 of the IPL in a pattern similar to that seen for type I and II cells.

The axonal fibers of type III cells emerged at dendritic branchpoints and were recognized easily by their small caliber (<1.0 μm diameter) and the regularly spaced large and small beads found throughout their lengths (Figs. 6A,C). Type III cells showed the most complex axonal arbor of all polyaxonal cells. The axonal segments often crossed, showed numerous branchpoints at which daughter segments could change direction dramatically from that followed by mother branches (Fig. 6C). The axonal

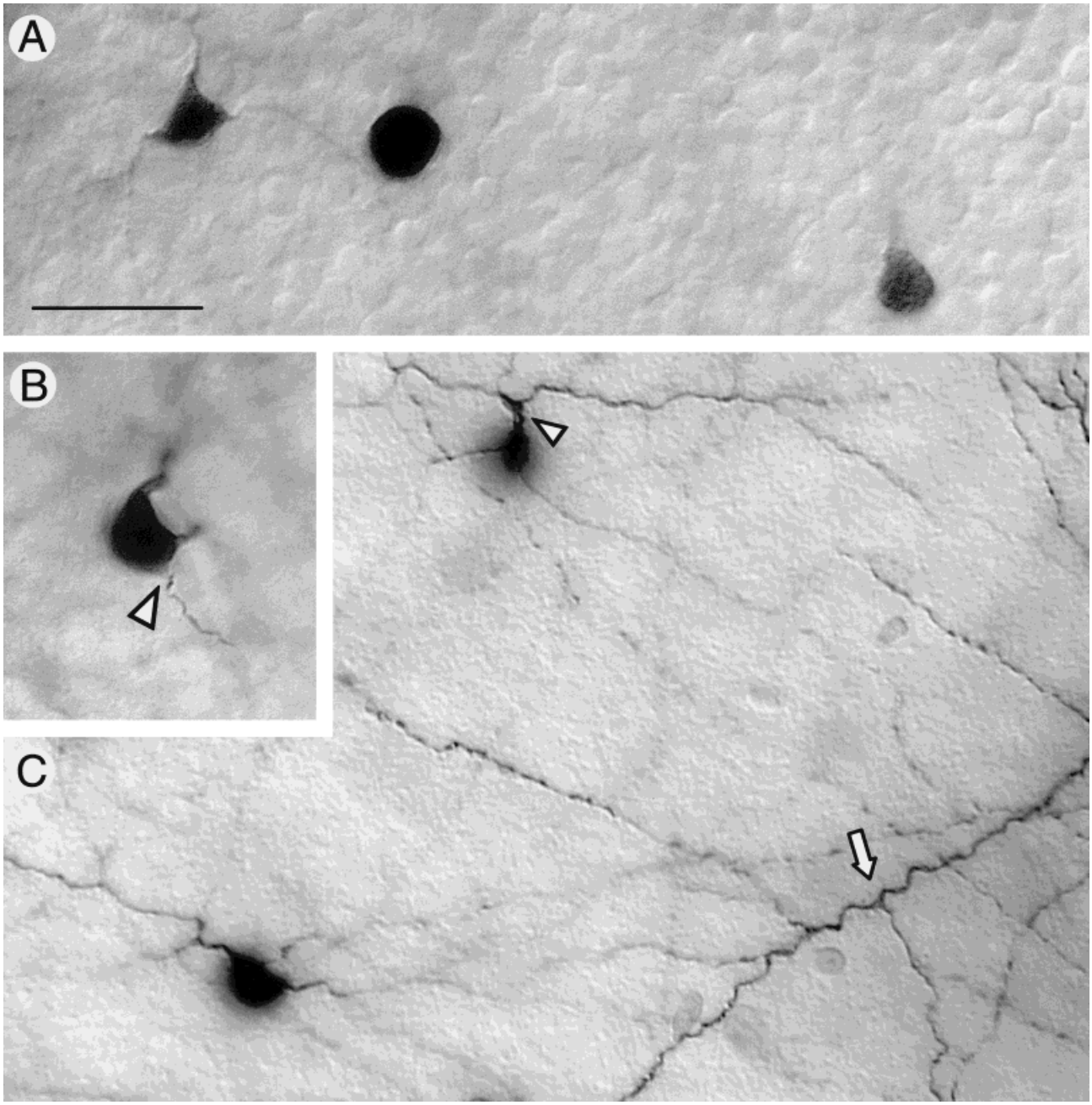

Fig. 3. **A:** Somata of tracer-coupled amacrine cells in the inner nuclear layer (INL) following the injection of a single type I polyaxonal cell. Cells showed clear differences in soma shape of labeling intensity, suggesting heterologous coupling. **B:** Type I polyaxonal cell soma in the inner plexiform layer (IPL) with a thin, axon-like process emerging directly from the cell body (arrowhead). **C:** Dendritic and axonal systems of tracer-coupled cells following injection of a type I polyaxonal cell with Neurobiotin. The arrowhead shows a main stalk emerging from the cell body of a tracer-coupled neuron, suggesting that it may be a type II polyaxonal cell tracer coupled to the injected type I cell. Arrow shows a branchpoint on the dendrite of a type I polyaxonal cell where an axonal process emerges. Scale bar = 25 μm.

arbor of type III cells ran for several millimeters within strata 2–4 of the IPL.

Type IV cells. Only two injections of type IV cells were made, suggesting that these may occur infrequently in the central rabbit retina. Again, extracellular accumulation of the peroxidase reaction product obscured the somata of injected cells. Therefore, it was necessary to infer the cell body size and shape from those of tracer-coupled cells. The somata of type IV cells were displaced to the GCL and were coupled to less than 10 cells laying in both the GCL and INL. Again, it is unclear whether the cells in the INL reflect heterologous coupling or a corresponding subset of type IV cells in the INL. The primary dendrites of type IV cells were relatively thin (1.0–1.2 μm in diameter) due to

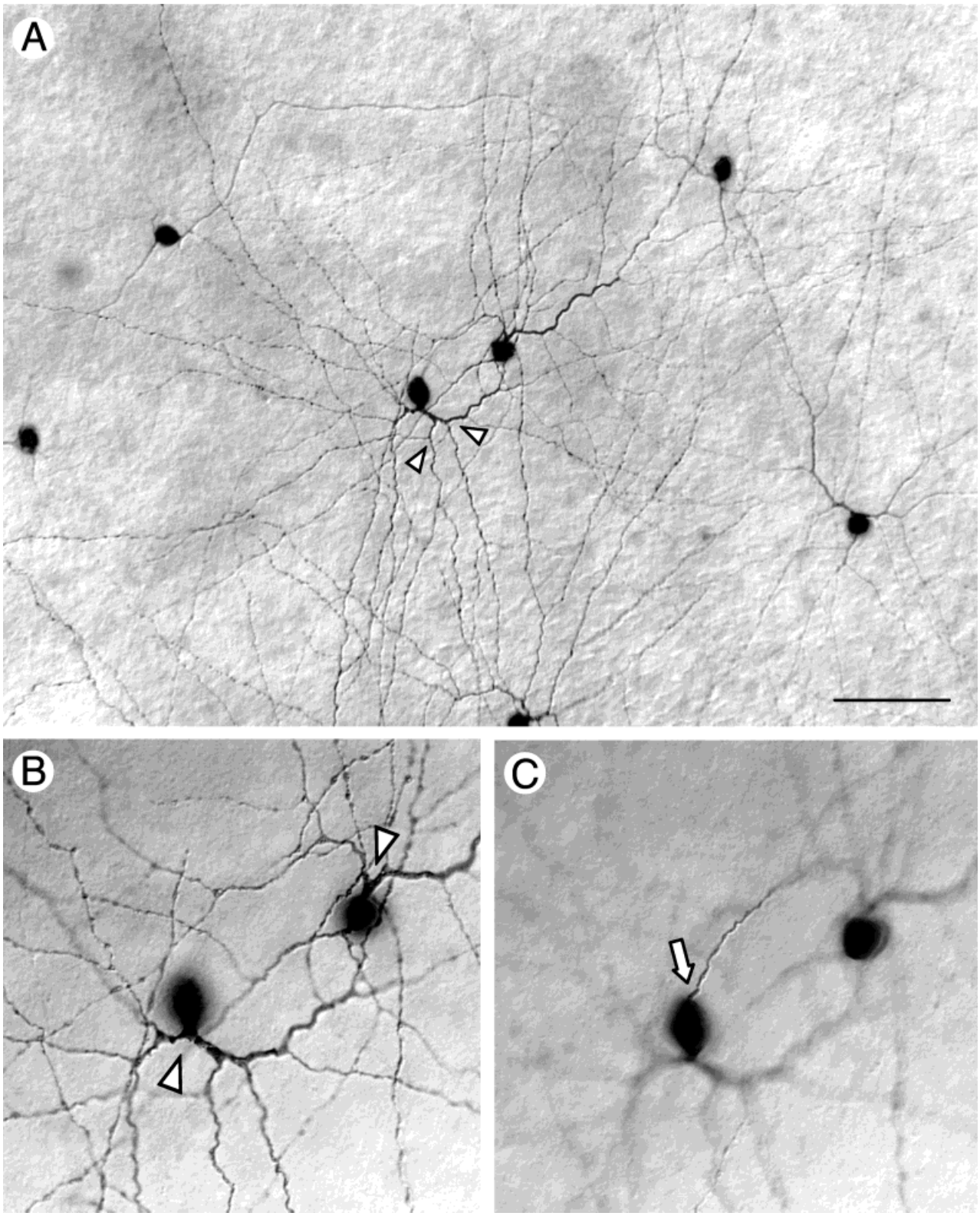

Fig. 4. **A:** Photomicrograph showing homologously coupled type II polyaxonal cells following the injection of one cell with Neurobiotin. Axonal processes often emerged from proximal dendrites at branchpoints (arrowheads). **B:** Type II polyaxonal cells showed distinctive thick main stalks that bifurcated in the middle of the IPL (arrowheads). **C:** Photomicrograph shows an axon emerging directly from the cell body of a type II cell (arrow); focal plane is the inner nuclear layer (INL)/inner plexiform layer (IPL) border. Scale bars = 50 μm in A, 25 μm in B,C.

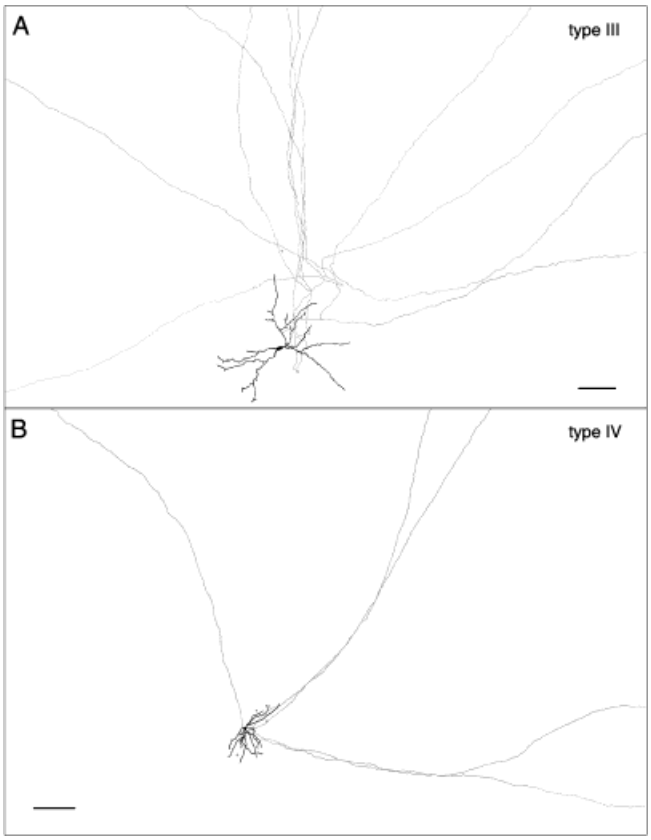

Fig. 5. **A:** Camera lucida drawing of a type III polyaxonal cell injected with Neurobiotin. The dendritic arbor is presented in black, whereas the extensive axonal system and tracer-coupled somata are in gray. **B:** Camera lucida drawing of a type IV polyaxonal cell labeled with Neurobiotin. Conventions are the same as in A.

the fact that they showed extensive tapering along their lengths. Dendrites showed numerous swellings and infrequent spines. The entire dendritic arbor of these cells showed only up to second-order branching and was 200–300 μm in diameter (Fig. 5B). Unlike the previously described polyaxonal amacrine cell types, the dendritic arbor of type IV cells stratified narrowly within stratum 4 of the IPL.

Long, unbranched axonal processes emerged from dendrites at branchpoints resulting in a sparse dendritic arbor (Fig. 5B). The axons were only slightly thinner (0.8–1.0 μm in diameter) than their dendritic counterparts. However, unlike the dendrites, they showed no tapering and could be traced distally for several millimeters until the staining faded completely. The axonal processes monostratified within stratum 4 of the IPL, slightly distal to the level of the dendritic processes.

Type V cells. The somata of type V cells were also displaced to the GCL and were tracer coupled to 10–20 cells in the GCL and INL. Variations in the soma size and labeling intensity of coupled cells suggested homologous as well as heterologous coupling to possibly two other types of amacrine cell (Fig. 8). The most distinguishing characteristic of type V cells was the dramatic elongation of their dendritic and axonal arbors along the axis parallel to the visual streak (Fig. 7A). The dendritic processes were wavy and showed numerous spines that ended in terminal boutons (Fig. 8). Most of the cells in this group had two, thick primary dendrites that ran in opposite directions to form a bipartite field, 250–350 μm in diameter. The dendritic processes ramified vitreally within strata 3–4 of the IPL.

Typically, thin, beaded axon-like processes emerged from dendritic branchpoints, but also appeared as direct extensions of dendritic terminal segments that narrowed rapidly. The axonal arbor showed little branching, but numerous crossings of individual segments were observed. Like the dendritic arbor, the axons formed an elongated, bipartite field (Fig. 7A). The axons stratified narrowly within stratum 4 of the IPL.

Type VI cells. Type VI polyaxonal cells lay in the proximal INL and displayed large, spherical cell bodies measuring about 14 μm in diameter (Fig. 9). Type VI cells showed the most extensive tracer-coupling pattern, typically composed of several hundred coupled cells (Figs. 7B, 9A). This pattern included a regular array of darkly labeled, homologously coupled cells as well as three types of heterologously coupled amacrine cells in the INL based on differences in soma size, shape, and labeling intensity (Fig. 9C). The pattern of tracer-coupled cells typically extended well beyond the dendritic field (250–300 μm diameter) of the injected cell (Fig. 7B). Three or four thick, wavy primary processes emerged from the cell body and branched proximally, resulting in long second and third-order terminal dendrites (Fig. 7B). Despite the curvy appearance of individual dendritic segments, the arbor maintained an overall radiate architecture with little overlap of individual branches. The surface of the primary dendrites was smooth, but higher-order segments displayed numerous swellings (Fig. 9B). The dendritic arbor of type VI cells ramified narrowly within stratum 3 of the IPL.

The axons of type VI cells usually emerged at dendritic branchpoints as well as extensions of dendritic processes that tapered quickly into finer axonal branches. The main axonal processes were either unbranched or branched proximally within 500 μm of the cell body and then ran for several millimeters (Fig. 7B). The axonal arbor stratified mainly within stratum 3 of the IPL, although processes were seen running distally for some of their extent within stratum 2.

A schematic summarizing the soma/dendritic/axonal morphologies and tracer-coupling patterns of the six types of polyaxonal cells is provided in Figure 10.

Physiology of polyaxonal amacrine cells

Type I cells. The light-evoked response of type I polyaxonal amacrine cells typically consisted of large, transient depolarizations, up to 25 mV in amplitude, and a corresponding increase in spike frequency at both stimulus onset and offset (Fig. 11). These cells also showed a high rate of spontaneous spike activity in the dark (Fig. 11A). Figure 11B shows the responses of a type I cell to concentric, centered spots of light of increasing diameter. Both focal and diffuse spot stimuli evoked clear on/off responses in this cell with highly similar waveforms. Analysis of these data provided a gross measurement of the cell's area summation for both the on/off responses of about 750–1,000 μm (Fig. 11C); although the on responses appear to show a somewhat smaller area summation than the off responses of this cell, we found this difference to be

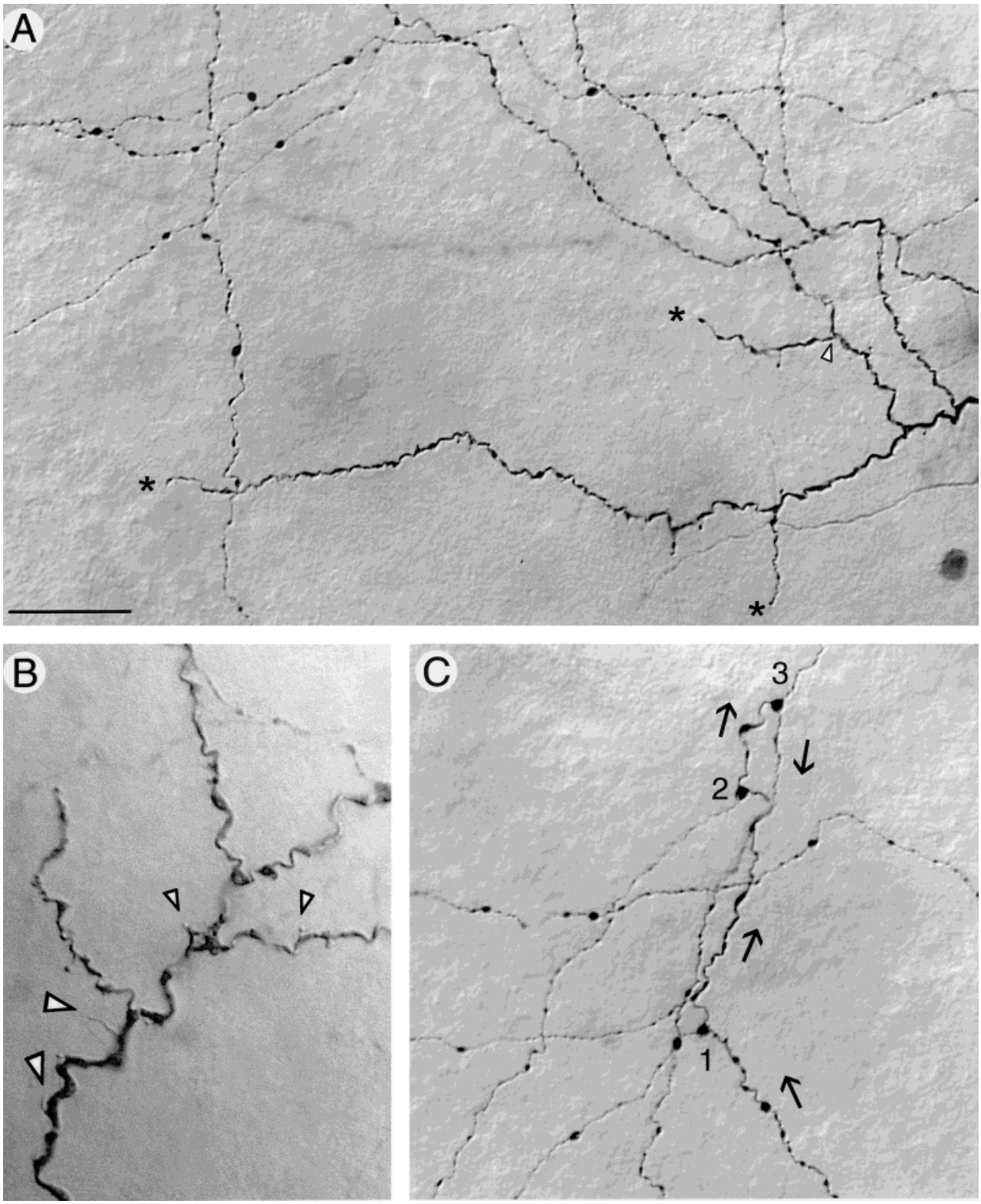

Fig. 6. **A:** Photomicrograph showing the dendritic and axonal architecture of a type III polyaxonal cell. The relatively thick dendrites showed numerous spines, whereas the axonal branches showed numerous large and small varicosities. **B:** The tortuous dendrites of type III cells showed numerous spines both with (small arrowheads) and without (large arrowheads) terminal heads. **C:** The axonal system of type III cells was extremely complex with daughter branches often dramatically changing direction. Numbers indicate the consecutive branchpoints of an axon arbor and arrows follow the distal flow of information. Scale bars = 25 μm in A, 12.5 μm in B, 25 μm in C.

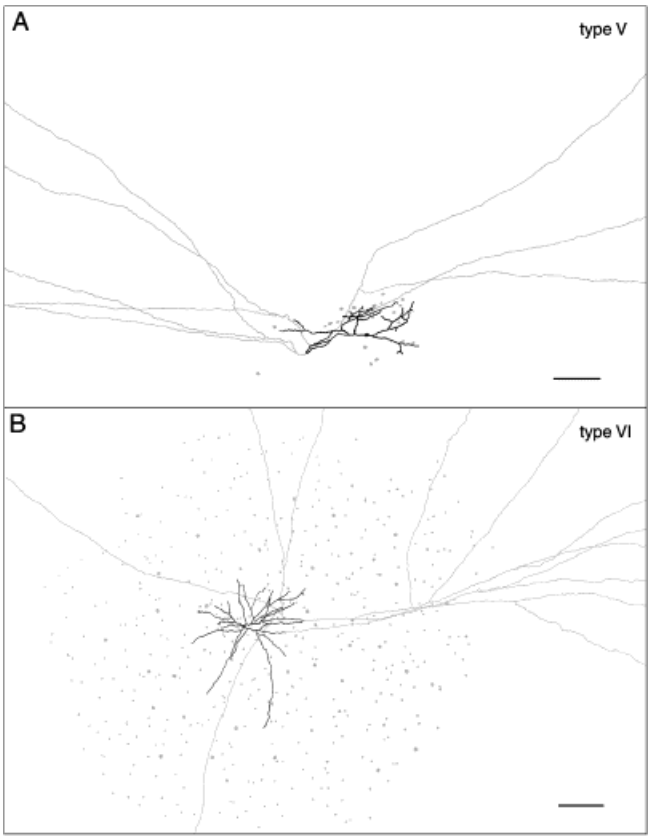

Fig. 7. **A:** Camera lucida drawing of the dendritic and axonal arbors of a type V polyaxonal cell injected with Neurobiotin. The dendritic arbor is presented in black, whereas the axonal arbor and tracer-coupled somata are in gray. Note the highly oriented profile of the arbors along the vertical axis (parallel to the visual streak). **B:** Camera lucida drawing of a type VI polyaxonal cell labeled with Neurobiotin. Conventions are the same as in A. Type VI cells showed the most extensive pattern of tracer coupling.

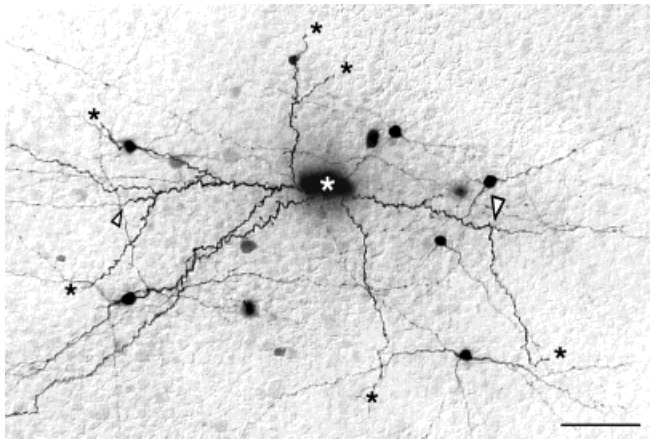

Fig. 8. Flatmount-view photomicrograph of type V polyaxonal amacrine cell labeled with Neurobiotin. The relatively thick dendritic processes ended (asterisks) proximally, whereas axonal processes emerged either from dendrites at branchpoints (large arrowhead) or directly from dendrites that tapered rapidly (small arrowhead). Scale bar = 25 μm.

variable across the population of type I cells and, on average, to be negligible. For this cell, illumination with more diffuse stimuli brought about a slight diminution in the amplitude of both the on/off responses, suggesting some suppressive influences from the far periphery. However, this response decrease to near full-field illumination was not seen in all cells. We recorded robust on/off responses to small spots of light displaced up to several hundred microns from the center of type I cells (Fig. 12A), suggesting that they maintain uniform on-off receptive fields without a conventional antagonistic surround.

To determine the size of the on/off receptive fields of type I cells, we measured responses to a narrow 50 μm-wide/6.0 mm-long slit of light that was displaced in discrete steps from the central position. Figure 12A shows the responses of a type I cell to such a stimulus paradigm. By comparing the relative peak response amplitude to stimulus displacement, the receptive field of both the on/off components was calculated as the diameter of the Gaussian functions fit to the data. For this cell, the on/off receptive fields were comparable in size: 367 vs. 395 μm; in general, type 1 cells showed coextensive on/off receptive fields (Fig. 12B). Further, the on/off receptive field of this cell was comparable to the cell's dendritic field size and thus was considerably smaller than its axonal arbor (Fig. 12B). This correspondence between a cell's receptive and dendritic field size is a theme that we found not only for type I cells, but for all the polyaxonal cell types we encountered in this study (see below).

Type II cells. Type II polyaxonal amacrine cells also displayed on/off responses that consisted of 5–10 mV depolarizations and transient bursts of spikes at light onset and offset (Fig. 13A). In contrast to type I cells, spontaneous action potentials were seen rarely in recordings from type II cells. The on-off responses were seen following presentation of both focal and diffuse stimuli, as well as small spots or slits of light presented throughout the receptive field. The area summation, as measured using concentric spots of light, averaged about 650 μm and was similar for both the on/off responses (Fig. 13A). In contrast to the type I cell responses described above, we saw no reduction in the amplitude of on/off responses of this cell to large spots of light. Type II cells therefore appeared to maintain uniform on-off receptive fields lacking an antagonistic surround.

Figure 13B shows a comparison of the peak on-off responses of a type II cell as a function of the position of a slit of light. The Gaussian functions fit to these data indicate an on receptive field of 260 μm and a corresponding off receptive field of 311 μm. These receptive field sizes matched closely to the extent of the cell's dendritic field diameter of 350 μm and were thus dwarfed by the axonal field of several millimeters (Fig. 13B). Similar to type I cells, the on/off receptive and dendritic field sizes of individual type II polyaxonal cells corresponded well.

Type III cells. The type III polyaxonal cells also showed on-off response activity. Like the cell types described above, type III cells showed large transient depolarizations and corresponding bursts of spike activity in response to the onset and offset of both focal and diffuse illumination. Although these cells clearly were capable of generating action potentials, they were never seen to arise spontaneously in the dark. Figure 13C shows the re-

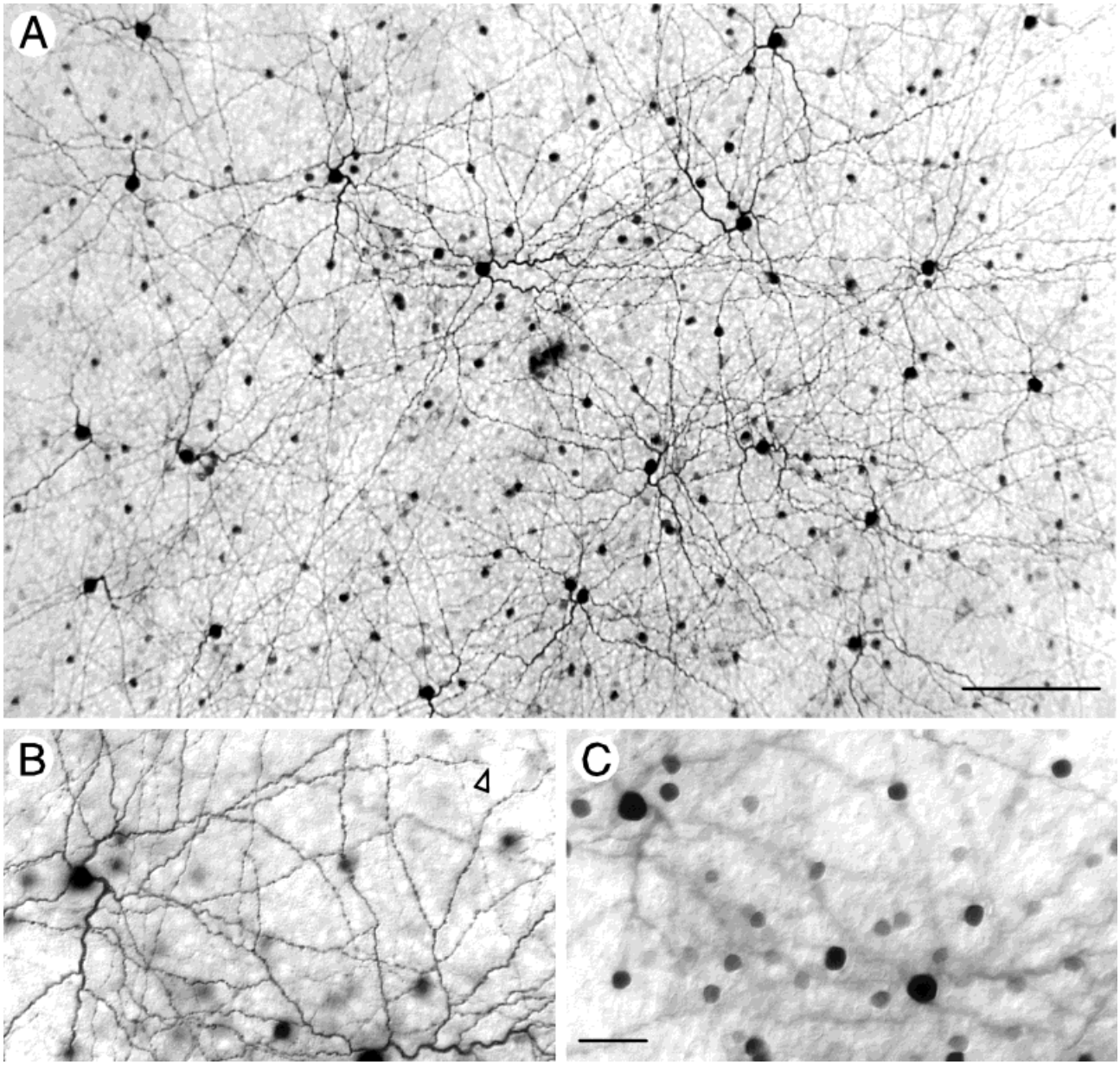

Fig. 9. **A:** Photomicrograph showing the extensive tracer- coupling pattern seen following injection of a single type VI polyaxonal cell with Neurobiotin. **B:** Both dendritic and axonal processes of type VI neurons ramified narrowly within stratum 3 of the inner plexiform layer (IPL). The arrowhead indicates a dendritic terminal ending. **C:** Photomicrograph of the somata tracer coupled to type VI cells. Differences in cell size and labeling intensity indicate heterologous coupling to at least three types of amacrine cell. Scale bars = 100 μm in A, 25 μm in B,C.

sponses of a type III cell to a 50 μm-wide/6.0 mm-long slit of light that was first centered over the cell (0 μm) and then displaced in discrete steps across the retina. Comparison of the on/off response amplitudes to stimulus position produced two curves that could be fit by Gaussian functions (Fig. 13D). The on-off receptive fields, taken as the diameter of the corresponding Gaussian functions, were 482 and 375 μm, respectively. Based on this type of analysis, type III cells generally showed on receptive fields that were about 10–20% larger than the off receptive fields. However, we were unable to find a position in which a peripherally placed light stimulus could evoke an on response in total isolation of the off response. Thus, in practice, the difference between the on/off receptive fields of these cells appeared negligible. Similar to the correspondences described for the other polyaxonal cell types, the extent of the on-off receptive field of an individual type III cell matched closely to the size of its dendritic arbor (Fig. 13D).

In summary, types I, II, and III polyaxonal amacrine cells all displayed uniform on-off receptive fields that matched the size of the corresponding dendritic arbors.

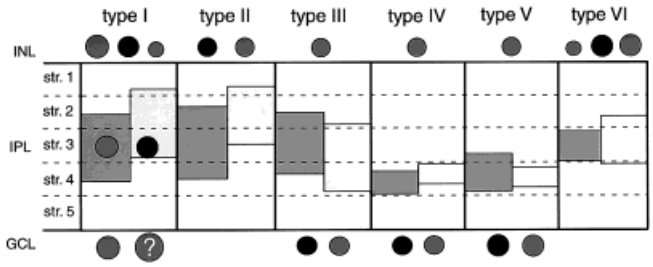

Fig. 10. Schematic summarizing the morphological features of the six polyaxonal cell types in the rabbit retina. The cell with the question mark under type I cells represents labeled ganglion cell somata for which physiological tracer coupling is equivocal (see text for details). Dark shaded areas, dendritic stratification; light shaded areas, axonal stratification; black circles, injected soma; shaded circles, tracer-couple soma.

The on-off responses of these cells were consistent with their dendritic/axonal arbors ramifying in both sublamina *a* and *b*, the respective off and on recipient zones of the IPL (Famglietti and Kolb, 1975; Bloomfield and Miller, 1986).

Type IV cells. In contrast to the previous cell types, type IV polyaxonal cells responded to focal (75 μm-diameter spot) stimulation with an on-center response consisting of a large, transient depolarization with a brief burst of spike activity riding at top, followed by a sustained phase that persisted for the entire stimulus period (Fig. 14A). Peripheral translation of the spot by 300 μm produced a sustained hyperpolarization reflecting an antagonistic off-surround (Fig. 14A). As aforementioned, we only encountered type IV cells on two occasions during the course of this study, suggesting that they occur infrequently in the central retina. Therefore, other than their on-center/off-surround physiology, we were unable to obtain information relating to the size of their receptive fields.

Type V cells. The type V polyaxonal amacrine cells responded to full-field illumination with a large amplitude, transient depolarization and a brief burst of spikes, followed by a more transient depolarization and spiking at light offset (Fig. 14B). However, presentation of a 75 μm-diameter spot of light produced an on-center response with waveform similar to that evoked in type IV cells. Lateral displacement of the spot by 300 μm produced a clear off-surround response consisting of a light-evoked hyperpolarization with transient and sustained components and a brief depolarization at light offset (Fig. 14B). Figure 14C shows a comparison of the peak response amplitude of a type IV cell to the position of a narrow slit of light displaced across the retina. The diameter of the Gaussian function fit to these data was 195 μm, which was somewhat smaller than the size of the cell's dendritic arbor, but clearly disparate from the enormous extent of its axonal arbor (Fig. 14D). Overall, like the other polyaxonal amacrine cell types, the extent of the on-center receptive fields of type IV cells corresponded well to that of their dendritic arbors.

Type VI cells. Type VI polyaxonal cells responded to both focal and diffuse stimuli with a transient depolarization and a burst of spikes riding at the top, followed by a rapidly falling phase with some intermediate spiking (Figs. 15A,B). The area summation of these cells averaged about 300 μm. Clear hyperpolarizing off-surround responses were not recorded in these cells. However, presentation of large spots of light (e.g., >375 μm in diameter) produced responses with considerably smaller amplitudes than those evoked by more focal stimuli, thus suggesting the presence of an antagonistic surround (Fig. 15A). Figure 15B shows the response of a type VI cell to a narrow slit of light first centered over the cell (0 μm) and than displaced across the retina in both directions. Data comparing the response amplitude to slit position could be fit with a Gaussian function with a diameter of 156 μm (Fig. 15C). The Gaussian diameter, taken as the extent of the cell's on-center receptive field, was considerably smaller in size than the cell's dendritic arbor. On average, however, the receptive fields of type VI cells were only about 15% smaller in size than their respective dendritic arbors.

In summary, type IV, V, and VI polyaxonal cells maintained on-center/off-surround receptive fields. The physiology of these cells was consistent with the finding that their dendritic/axonal arbors ramified exclusively, with the exception of some type VI cell axonal fibers, within sublamina *b* of the IPL.

DISCUSSION

The polyaxonal amacrine cell has emerged relatively recently as a clearly identifiable class of retinal neuron. The distinctive characteristic of these cells is the discrete dendritic and axonal arbors that constitute largely separate branching structures. In this study, we were able to recognize six types of polyaxonal cells based on clear differences in soma/dendritic/axonal architecture and tracer-coupling patterns. Our results confirm and extend the earlier reports by Famiglietti (1992a,b,c), who described four types, that polyaxonal cells in the rabbit retina form a morphological heterogeneous group. Likewise, we also found that polyaxonal cells express a number of different response properties related to their on/off receptive fields, response waveform, and both light-evoked and spontaneous spike activities. Taken together, our results suggest that the different polyaxonal cell types are not simply variations of a central morphological theme, but reflect cell groups that perform different functional roles in the retina.

Comparison with other morphological studies

There have been numerous morphological and immunocytochemical studies of polyaxonal amacrine cells in the mammalian retina. As aforementioned, Famiglietti (1992a,b,c) performed the most comprehensive study of the polyaxonal types in the rabbit. Below, we discuss the correspondence between the six classes of polyaxonal amacrine cells described here and those reported by Famiglietti in rabbit as well as the polyaxonal cell types described in other species.

The type I polyaxonal cell we classified likely corresponds to the PA1 neuron described by Famiglietti (1992a). The somata of both these neuronal populations lay in the INL or were displaced to the GCL, but mostly within the IPL. Both cell types share a number of morphological features in common, including soma size and shape, tortuous dendritic branches, highly branched ax-

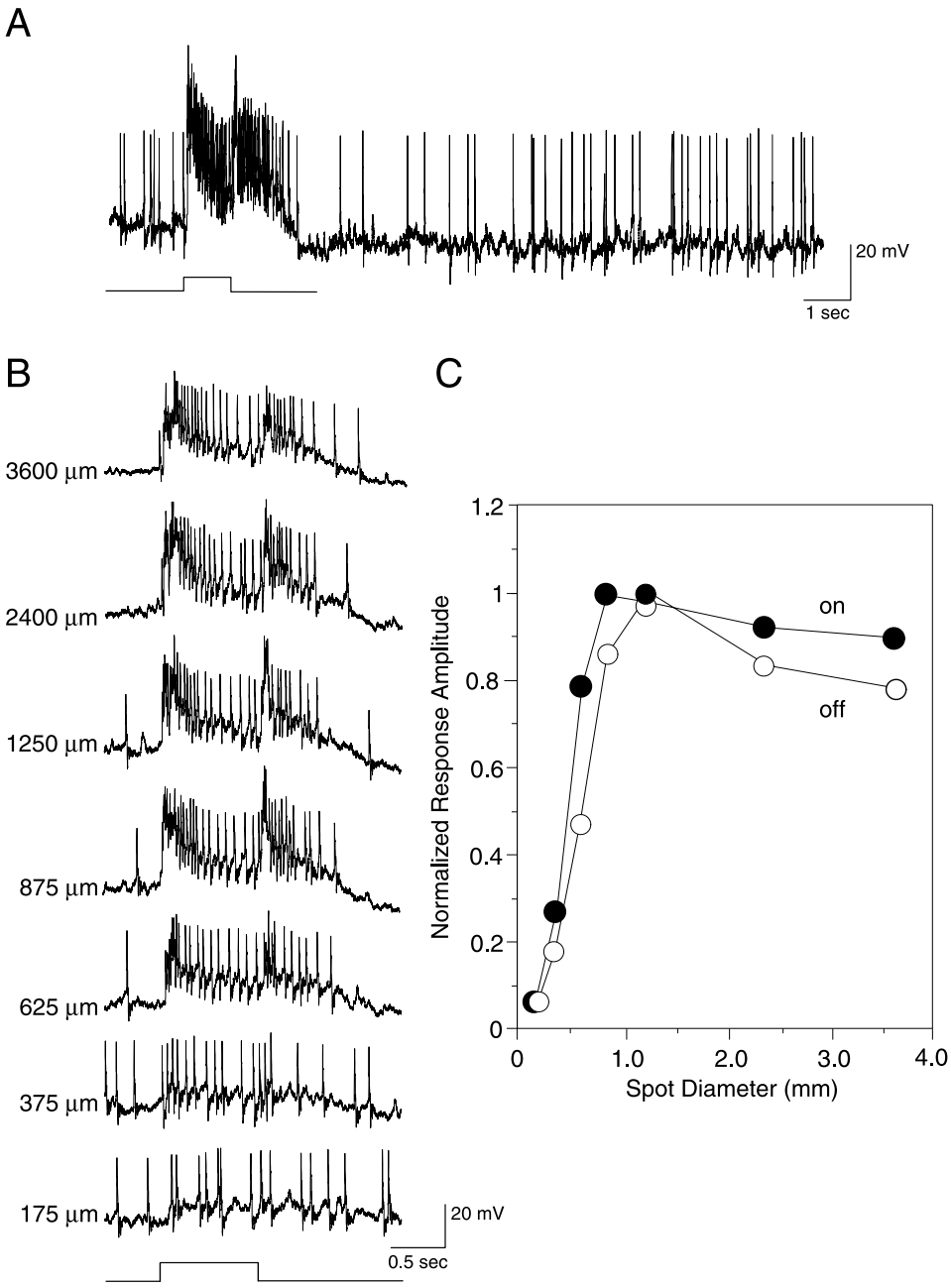

Fig. 11. Light-evoked responses of a type I polyaxonal cell . Light trace below each group of recordings indicates the onset and offset of the light stimulus. Light intensity = -5.5 log units. **A:** Light-evoked response to full-field illumination includes large depolarizations and increased spike activity at both light onset and offset. **B:** Responses evoked by concentric spots of light of varying sizes centered over the soma; value to the left of each trace indicates spot diameter. **C:** Comparison of the relative peak response amplitude and stimulus diameter based on the data in B. Area summation of this cell was 750–1,000 µm. Although there is some amplitude reduction to large stimuli, this was not seen in all cells.

onal arbors, and dendritic/axonal stratification mainly within strata 2–4 of the IPL. In a comparison with other species, the type I polyaxonal cell corresponds most closely to the A22 cell of the cat retina (Kolb et al., 1981). The A22 cells also have cell bodies in the INL, GCL, or within the neuropil of the IPL. They also show thick, curvy dendrites as well as thinner beaded axon-like processes that stratify within both sublamina *a* and *b*; the A22 cells also appear to have on-off responses (Freed et al., 1996). In primates, Stafford and Dacey (1997) described the A1 polyaxonal cell that also appears homologous to our type I cell. Both cell types show large somata located in the INL, GCL, or IPL, a highly branched, circumscribed dendritic arbor, and an expansive axonal arbor made up of thin, beaded processes; the dendritic/axonal arbor of A1 cells also stratifies within the middle of the IPL. The A1 amacrine cells display on-off light-evoked responses very similar in waveform to those of type I cells. In addition, both cell types display receptive fields slightly larger in size than their respective dendritic diameters. Finally, both cells are coupled to an extensive array of somata within all three layers (INL, IPL, GCL). One clear difference, however, is that A1 cells in the macaque retina are tracer coupled to a class of medium-size ganglion cells, whereas we did not observe ganglion cells that were clearly tracer coupled to type I cells in the rabbit retina. As aforementioned, we did see labeled ganglion cell somata following injection of Neurobiotin into type I cells, but these were very close to

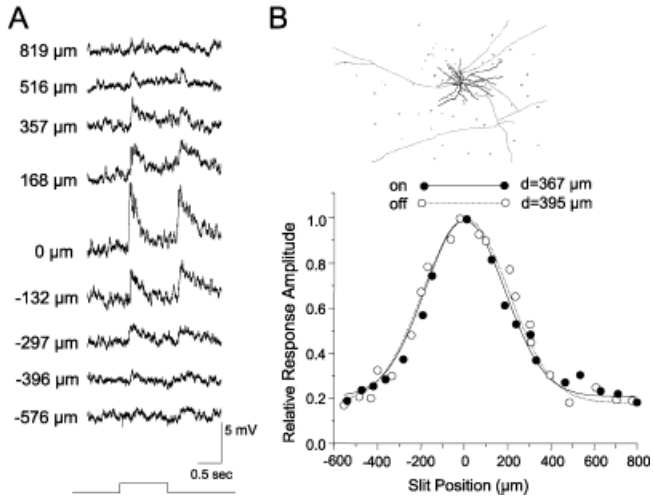

Fig. 12. Receptive field properties of a type I polyaxonal cell. **A:** Receptive field measurements were made with a 50 µm-wide/6.0 mm-long slit of light that was moved in steps across its minor axis. The value to the left of each trace indicates how far the slit was moved from the central position (0 µm). Measurements were made of slow potential amplitudes after spike activity had ceased spontaneously. Light intensity = log -5.5. **B:** The extent of the cell's receptive field was calculated as the diameter of the Gaussian function fit to the peak amplitudes of the response data in A (bottom). The on/off receptive fields were approximately coextensive and matched well to the size of the cell's dendritic arbor. Drawing of the cell is shown at the top; dendrites are presented as black, whereas the axonal arbor (only the very proximal portion is shown) and the tracer-coupled somata are in gray. The magnification of the drawing coincides to that of the horizontal bars below representing the extent of the on/off receptive fields.

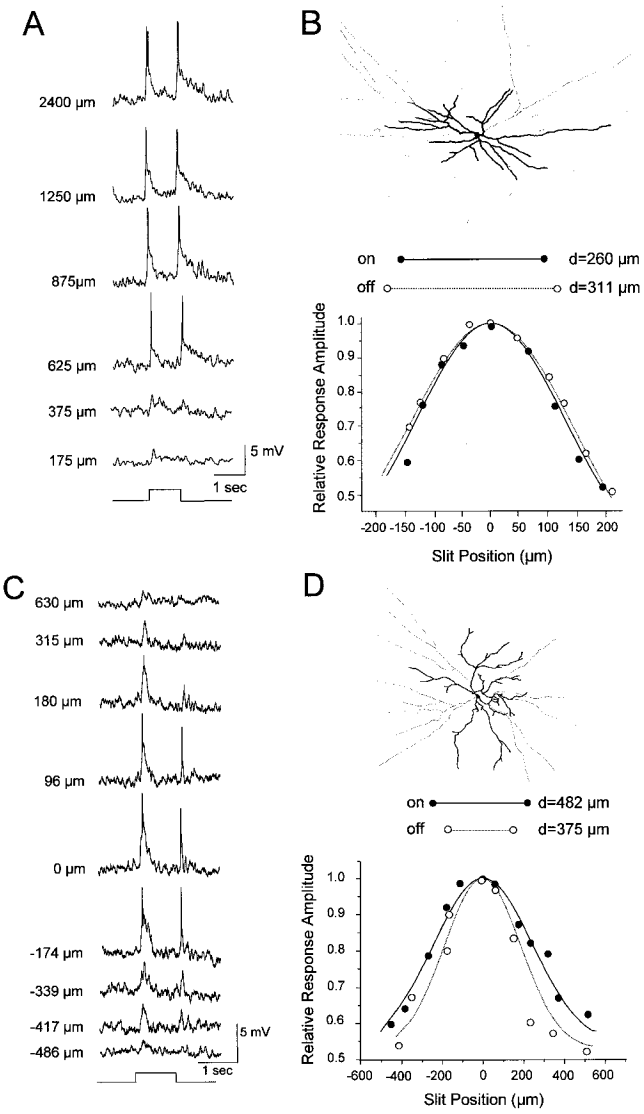

Fig. 13. Response properties of type II and III polyaxonal cells. Both type II and type III neurons displayed depolarizations at light onset and offset as well as transient burst of spikes. **A:** Responses of a type II cell evoked by concentric spots of light of varying sizes centered over the soma of a type II cell. Values to the left of each trace indicate the diameter of the spot stimulus. Type II cells displayed uniform on-off receptive fields without antagonistic surrounds. **B:** A comparison of relative response amplitude to the position of a 50 µm-wide/6.0 mm-long slit stimulus. Conventions are the same as in Figure 12B. Both the on/off receptive fields of this type II cell matched closely to the size of its dendritic field. **C:** Responses of a type III polyaxonal cell to the slit of light first centered over the cell (0 µm) and then displaced distally. Conventions are the same as in Figure 12A. **D:** The on/off receptive fields were calculated as the diameters of the Gaussian functions fit to the data comparing peak response amplitude to slit position. Although the off receptive field of type III polyaxonal cells appeared to be slightly smaller than that of the on receptive field, they still matched closely the size of the corresponding dendritic field. Conventions are the same as in Figure 12B.

the injection site and thus appeared to reflect random labeling due to tracer leakage than true tracer coupling through gap junctions.

In the Golgi studies of retinal amacrine cells (Kolb et al., 1981; Kolb et al., 1992; Famiglietti, 1992a,b,c), we found none that clearly correspond to our type II polyaxonal cells. Famiglietti reported only a single cell type with cell bodies in the INL, the PA4 cells, but the arborizations of these neurons were restricted to stratum 1 and not strata 2–4 as seen for our type II cells. The closest cell type in the cat retina is the A21 amacrine cell that maintains a wide dendritic field (the authors did not separate the arbor into dendritic and axonal zones) that is formed from a single primary stalk (Kolb et al., 1981). However, the arbors of A21 cells were reported to stratify deep in the IPL within stratum 5. Although the wiry type 2 amacrine cell in humans shows a soma/dendritic morphology similar to that of type II cells in the rabbit, including a thick main stalk, and smooth, straight primary dendrites, their cell bodies are displaced to the GCL (Kolb et al., 1992).

Overall, the type II polyaxonal cells appear to correspond best to the NADPH-diaphorase-positive neurons in the rabbit, rat, cat, and human retinas (Sandell, 1985; Sagar, 1986). These neurons display ovoid cell bodies in the INL that emit a primary dendritic stalk that bifurcates into an expansive arborization stratifying in the middle of the IPL. Recently, we have shown that the NADPH-diaphorase amacrine cells in the rabbit express the phosphorylated neurofilament-H epitope localized to central nervous system (CNS) axons, thus identifying them as axon-bearing amacrine cells (Völgyi and Bloomfield, 2001).

The type III polyaxonal cells correspond closely to the PA2 neurons described in the Golgi-impregnated rabbit

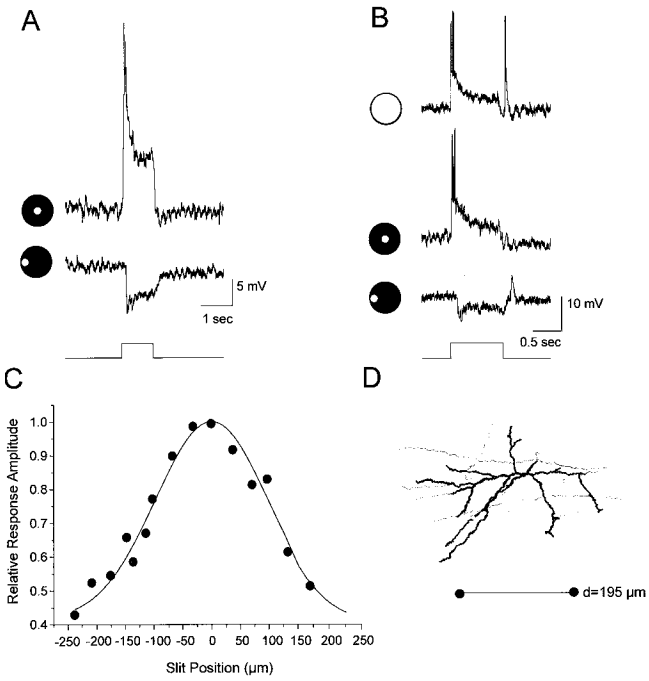

Fig. 14. **A:** Responses of a type IV polyaxonal cell to a 75 μm-diameter spot of light centered over the cell (top) and then displaced laterally by 300 μm (bottom). **B:** Light-evoked responses of a type V polyaxonal cell to full-field illumination (top) and to a 75 μm-diameter small spot of light centered over the cell (middle) and displaced laterally by 300 μm (bottom). **C:** Gaussian function fit to data comparing response amplitude and the position of a slit light stimulus. The on receptive field of this type V polyaxonal cell matched well to the size of its dendritic arbor. Conventions are the same as in Figure 12.

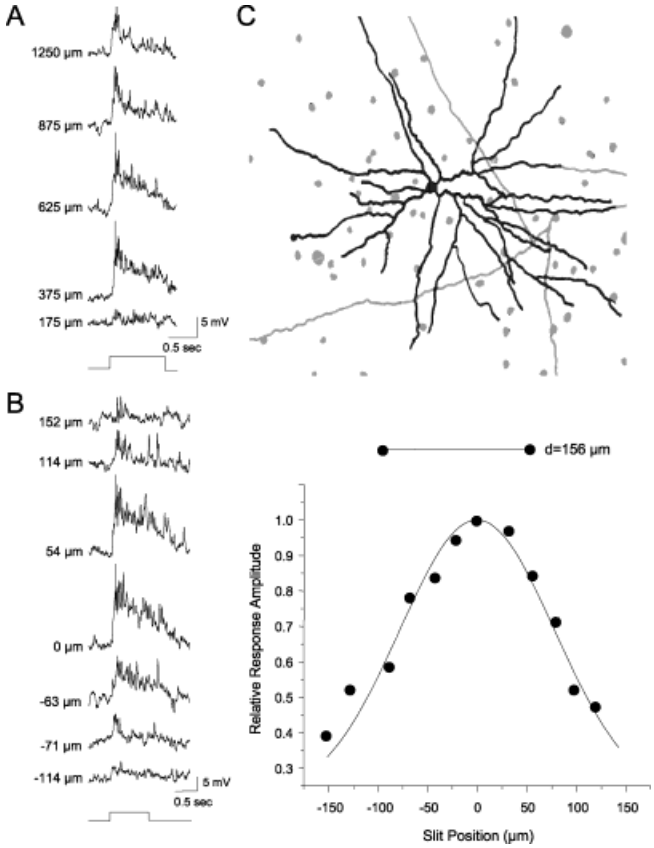

Fig. 15. **A:** On-center responses of a type VI polyaxonal cell to concentric spots of light of increasing size. Note that responses to large spots are diminished presumably due to activation of an antagonistic off-surround. Conventions are the same as in Figure 11A. **B:** A Gaussian function fit to a comparison of response amplitude to the position of a slit light stimulus. The on-center receptive field of the type VI cell, taken as the diameter of the Gaussian function, was somewhat smaller than its dendritic arbor. Conventions are the same as in Figure 12.

retina (Famiglietti, 1992c). Both neuronal types maintain somata in the GCL and have irregular, curvy dendrites with numerous swellings, spines, and boutons. One difference between these cell types is that PA2 cell arbors stratify mainly at the strata 4–5 border, whereas type III cells stratify more broadly from stratum 2 to the strata 4–5 border. The type III cells also share several morphological similarities with the Golgi-labeled thorny type 2 neurons in the human (Kolb et al., 1992) and monkey (Mariani, 1990) retinas. Like type III cells, these neurons have somata in the GCL, spiny dendritic processes, and arbors stratifying in the middle of the IPL.

We found no mammalian amacrine cells reported in the literature that displayed morphology similar to that of the type IV polyaxonal amacrine cell in the rabbit (Kolb et al., 1981, 1992; Mariani, 1990; Famiglietti, 1992a,b,c). More recently, Taylor (1996) labeled two long-range, axon-bearing amacrine cells in the rabbit retina. Although morphological descriptions were limited, one of the cells shares some properties in common with our type IV cell including thin, wavy dendrites and unbranched axons. This cell also showed on-center/off-surround physiology similar to that described here for type IV cells.

In some respects, our type V polyaxonal cell resembles a subtype of PA3 neurons described by Famiglietti (1992c) in the rabbit retina. In addition to similarities in soma size, location, and shape, both neuronal types maintain thick dendritic processes densely packed with spines and short side-appendages. Although most PA3 neurons were reported to be multistratified in strata 1,3, and 4, one subtype showed processes ramifying predominantly in stratum 4 as described for type V cells. A striking characteristic of type V cells was the elongated dendritic/axonal profile along the axis parallel to the visual streak. Famiglietti (1992c) described a variety of PA3 cells with a similar asymmetric architecture (see Fig. 5a,b of that paper).

We found no Golgi or Nissl-labeled mammalian amacrine cells in the literature that corresponded to the type VI polyaxonal cells in the rabbit. Again, Famiglietti (1992c) reported only one class of rabbit polyaxonal cell type (PA4) with somata in the INL. However, PA4 cells stratified within the very distal IPL, in stratum 1, whereas the arbors of type VI cells ramified in stratum 3. Further, the PA4 cells showed numerous dendritic spines, whereas processes of type VI cells were relatively smooth.

Response properties

The polyaxonal cells types in this study could be divided equally into on-off (types I–III) and on-center cells (types

IV–V1). Receptive field measurements from individual on-off cells indicated that their on/off receptive fields were largely coextensive, ranging from 350 to 700 μm in the central retina. In contrast, on-center polyaxonal cells showed classic, antagonistic off-surround receptive fields. As a result, on-center cells showed center-receptive field diameters of only 250–350 μm. These findings extend recent studies of the physiology of polyaxonal cells in a number of mammalian retinas. In the rabbit, Taylor (1996) recorded from only two polyaxonal cells, but found both to have on-center/off-surround receptive fields. Although the morphological descriptions of those cells were limited, based on the drawings provided (Fig. 1 of that paper), it would appear they correspond to our type IV and V cells. In contrast, polyaxonal amacrine cells in the macaque and cat have been recorded with on-off responses (Freed et al., 1996; Stafford and Dacey, 1997). As those studied focused on a limited number of cell types, the AI in the monkey and the A19 and A22 in the cat, it is possible that other polyaxonal cell types in both species may also show on-center responses as well.

Interestingly, we found that the on/off physiology of individual cells corresponded to their sublamina stratification pattern in the IPL. That is, on-off cells displayed dendritic and axonal arbors branching in both sublamina *a* and *b*, whereas on-center cells maintained arbors restricted to sublamina *b*. This means that both dendritic and axonal arbors are positioned to receive the appropriate bipolar cell input. Although no recordings to date have revealed an off-center polyaxonal cell response, Famiglietti (1992c) described PA3 and PA4 subtypes in the rabbit retina, some of which maintained a sizeable portion of their dendritic arbors in sublamina *a*. Most of the PA3 subtypes appear to correspond to our type V cells (see below). Clearly, we did not encounter the variety with processes in sublamina *a* as described by Famiglietti. The type PA4 cells correspond most probably to the TH-IR (dopaminergic) amacrine cells, whose dendrites stratify mainly in stratum 1 (Dacey, 1990; Famiglietti, 1992c). Finally, Vaney et al. (1988) described a subpopulation of neurofibrillar-stained amacrine cells with multiple axon-like processes that stratify within stratum 2 in the outer IPL. Therefore, it is plausible that off-center polyaxonal cells exist, but a combination of low cellular density and electrode bias has precluded recording of them.

Correlation between dendritic and receptive field size

A robust finding for all the polyaxonal cell types in the rabbit retina was that their receptive fields were comparable in size to their corresponding dendritic fields and thus significantly smaller than their expansive axonal arbors. Interestingly, in comparison with their respective dendritic diameters, the receptive fields of cell types I–III were slightly larger in size, whereas the receptive fields of cell types IV–VI were slightly smaller. These data probably reflect the fact that the latter types showed antagonistic surrounds whereas the former types displayed uniform on/off receptive fields. Further, this correspondence occurred even for cell types I and VI that showed extensive tracer coupling. These results confirm a previous finding in our lab that the receptive fields of inner retinal neurons generally are not enlarged by electrical coupling with neighboring cells (Xin and Bloomfield, 1999).

The correspondence between dendritic and receptive field size confirms and extends findings from prior studies of polyaxonal cells in the mammalian retina (Taylor, 1996; Stafford and Dacey, 1997). One exception to this rule appears to occur in the cat retina, in which Freed et al. (1996) reported polyaxonal cells with on/off receptive fields that extended well beyond their dendritic arbors. However, in that study, the receptive fields were computed by multiplying the Gaussian diameters values by three. Without this multiplication factor, the receptive and dendritic fields of cat polyaxonal cells match well and thus support findings in other mammalian retinas, including the present data from the rabbit.

The most parsimonious explanation for the correspondence between receptive and dendritic field size is that the excitatory drive to polyaxonal cells is restricted locally to the dendritic arbor. In this scheme, the large axonal arbor would serve as a transmitting zone to propagate this signal to distant areas across the retina. In this regard, polyaxonal cells in the rabbit retina showed clear evidence of regenerative action potentials as has been shown previously for certain polyaxonal cells in other mammalian retina (Freed et al., 1996; Taylor, 1996; Stafford and Dacey, 1997). We conclude that the spike discharge is a common feature of all polyaxonal neurons in the mammalian retina, presumably underlying the centrifugal propagation of signals across the extensive axonal arbor. It should be noted that the area summation of an individual polyaxonal cell generally was much larger than its receptive fields. However, this was a gross measure, based on stimulation with only a few concentric spot diameters. Therefore, conclusions about whether they reflect innervation peripheral to the center-innervation cannot be made.

Spike propagation

Interestingly, Stafford and Dacey (1997) and Famiglietti (1992c) have described axon hillock-like structures at the point at which axons emerge from primary dendrites that could reflect spike initiation sites. In our recordings, all spikes appeared to be large-amplitude somatic spikes (Miller and Dacheux, 1976). In contrast to recordings from cat polyaxonal cells (Freed et al., 1996), we never observed small-amplitude dendritic or possibly back-propagating axonal spikes. These data provide further evidence that regenerative spike transmission is orthograde and unidirectional.

However, for type V and VI polyaxonal cells, we found that axons sometimes emerged from the distal endings of dendrites rather than from the proximal segments. This presents the interesting question: Do synaptic inputs move centrifugally to initiate spikes first at an axon hillock at the axonal/dendritic junctures or centripetally to initiate spikes first at the soma that are then transmitted distally to all axons? These alternatives could allow for independent signaling in individual axons in the first case, but a more global distribution of signals to all axons in the latter. Support for the latter alternative comes from the fact that polyaxonal cells appear to release a number of neuromodulators, including dopamine (Dacey, 1990; Tauchi et al., 1990) nitric oxide (Sandell, 1985; Sagar, 1986; Perez et al., 1995), and peptides (Sagar, 1987; Cuenca et al., 1995; Rickman et al., 1996), for which the axonal output would appear to provide a more global signal to modulate gross activity across the retina rather than spa-

tially precise signaling. This would suggest that the expansive axonal arbors of polyaxonal cells probably act most often as a unit, distributing the same signals to several distant zones within the retina, rather than as independent structures carrying different visual information.

ACKNOWLEDGMENTS

Supported by NIH grant EY07360 (S.A.B.), NIH Postdoctoral Fellowship EY06689 (D.X.), a Postdoctoral Fellowship from the Fight for Sight Research Division of Prevent Blindness America (B.V.), and the Sackler Institute for Graduate Biomedical Sciences (Y.A.)

LITERATURE CITED

Bloomfield SA. 1992. Relationship between receptive and dendritic field size of amacrine cells in the rabbit retina. J Neurophysiol 68:711–725.

Bloomfield SA, Miller RF. 1982. A physiological and morphological study of the horizontal cell types in the rabbit retina. J Comp Neurol 208:288–303.

Bloomfield SA, Miller RF. 1986. A functional organization of ON and OFF pathways in the rabbit retina. J Neurosci 6:1–13.

Bloomfield SA, Xin D, Persky SE. 1995. A comparison of receptive field and tracer coupling size of horizontal cells in the rabbit retina. Vis Neurosci 12:985–999.

Cuenca N, De Juan J, Kolb H. 1995. Substance P-immunoreactive neurons in the human retina. J Comp Neurol 356:491–504.

Dacey DM. 1989. Axon-bearing amacrine cells of the Macaque monkey retina. J Comp Neurol 284:275–293.

Dacey DM. 1990. The dopaminergic amacrine cells of cat retina. Invest Ophthalmol Vis Sci 31:S535.

Famiglietti EV. 1992a. Polyaxonal amacrine cells of rabbit retina: morphology and stratification of PA1 cells. J Comp Neurol 316:406–421.

Famiglietti EV. 1992b. Polyaxonal amacrine cells of rabbit retina: size and distribution of PA1 cells. J Comp Neurol 316:406–421.

Famiglietti EV. 1992c. Polyaxonal amacrine cells of rabbit retina: size and distribution of PA2, PA3, and PA4 cells. Light and electron microscopic studies with a functional interpretation. J Comp Neurol 316:422–446.

Famiglietti EV, Kolb H. 1975. A bistratified amacrine cell and synaptic circuitry in the inner plexiform layer of the retina. Brain Res 84:293–300.

Freed MA, Pflug R, Kolb H, Nelson R. 1996. ON-OFF amacrine cells in cat retina. J Comp Neurol 364:556–566.

Kolb H, Nelson R, Mariani A. 1981. Amacrine cells, bipolar cells and ganglion cells of the cat retina: a Golgi study. Vision Res 21:1081–1114.

Kolb H, Linberg K, Fisher SK. 1992. Neurons of the human retina: a Golgi study. J Comp Neurol 318:147–187.

MacNeil MA, Heussy JK, Dacheux RF, Raviola E, Masland RH. 1999. The shapes and numbers of amacrine cells: matching of photofilled with Golgi-stained cells in the rabbit retina and comparison with other mammalian species. J Comp Neurol 413:305–326.

Mariani AP. 1990. Amacrine cells of the rhesus monkey retina. J Comp Neurol 301:382–400.

Miller RF, Dacheux R. 1976. Dendritic and somatic spikes in mudpuppy amacrine cells: identification and TTX sensitivity. Brain Res 104:157–162.

Miller RF, Bloomfield SA. 1983. Electroanatomy of a unique amacrine cell in the rabbit retina. Proc Natl Acad Sci USA 80:3069–3073.

Perez MTR, Larsson B, Alm P, Andersson K-E. 1995. Localization of neuronal nitric oxide synthase-immunoreactivity in rat and rabbit retinas. Exp Brain Res 104:207–217.

Ramón y Cajal S. 1893. La retine des vertebrates. Cellule 9:121–225. Thorpe SA, Glickstein M, Trans. Springfield: Charles C. Thomas, 1972.

Rickman DW, Blanks JC, Brecha NC. 1996. Somatostatin-immunoreactive neurons in the adult rabbit retina. 365:491–503.

Rodieck RW. 1988. The primate retina. In: Steklis HD, Erwin J, editors. Comparative primate biology, Vol. 4. Neuroscience. New York: Alan R. Liss. p 203–278.

Sagar SM. 1986. NADPH diaphorase histochemistry in the rabbit retina. Brain Res 373:153–158.

Sagar SM. 1987. Somatostatin-like immunoreactive material in the rabbit retina: immunohistochemical staining using monoclonal antibodies. J Comp Neurol 266:291–299.

Sandell JH. 1985. NADPH diaphorase cells in the mammalian inner retina. J Comp Neurol 238:466–472.

Stafford DK, Dacey DM. 1997. Physiology of the A1 amacrine: a spiking, axon-bearing interneuron of the macaque monkey retina. Vis Neurosci 14:507–522.

Tauchi M, Madigan NK, Masland RH. 1990. Shapes and distributions of the catecholamine-accumulating neurons in the rabbit retina. J Comp Neurol 293:178–189.

Taylor WR. 1996. Response properties of long-range axon-bearing amacrine cells in the dark-adapted rabbit retina. Vis Neurosci 13:599–604.

Vaney DI. 1990. The mosaic of amacrine cells in the mammalian retina. In: Osborne NN, Chader J, editors. Progress in retinal research, Vol. 9. Oxford: Pergamon. p 49–100.

Vaney DI, Peichl L, Boycott BB. 1988. Neurofibrillar long-range amacrine cells in mammalian retinae. Proc R Soc Lond [Biol] 235:203–219.

Völgyi B, Bloomfield SA. 2001. Axonal neurofilament-H immunolabeling in the mammalian retina. Invest Ophthal Vis Sci 42:S674.

Wässle H, Boycott BB. 1991. Functional architecture of the mammalian retina. Physiol Rev 71:447–480.

Xin D, Bloomfield SA. 1999. Comparison of the responses of AII amacrine cells in the dark- and light-adapted rabbit retina. Vis Neurosci 16:653–665.